

Direct observation of exchange-driven spin interactions in one-dimensional system

Chengyu Yan, Sanjeev Kumar, Kalarikad Thomas, Michael Pepper, Patrick See, Ian Farrer, David Ritchie, J. P. Griffiths, and G. A. C. Jones

Citation: *Appl. Phys. Lett.* **111**, 042107 (2017); doi: 10.1063/1.4989374

View online: <http://dx.doi.org/10.1063/1.4989374>

View Table of Contents: <http://aip.scitation.org/toc/apl/111/4>

Published by the [American Institute of Physics](#)

Articles you may be interested in

[Single shot ultrafast all optical magnetization switching of ferromagnetic Co/Pt multilayers](#)

Applied Physics Letters **111**, 042401 (2017); 10.1063/1.4994802

[Enhanced ultrasonic focusing and temperature elevation via a therapeutic ultrasonic transducer with sub-wavelength periodic structure](#)

Applied Physics Letters **111**, 053701 (2017); 10.1063/1.4990772

[Active tuning of high-Q dielectric metasurfaces](#)

Applied Physics Letters **111**, 053102 (2017); 10.1063/1.4997301

[The limit of quantum cascade detectors: A single period device](#)

Applied Physics Letters **111**, 061107 (2017); 10.1063/1.4985711

[Ferromagnetism in graphene due to charge transfer from atomic Co to graphene](#)

Applied Physics Letters **111**, 042402 (2017); 10.1063/1.4994814

[Degradation-induced low frequency noise and deep traps in GaN/InGaN near-UV LEDs](#)

Applied Physics Letters **111**, 062103 (2017); 10.1063/1.4985190



CiSE is already at
your fingertips...



In the IEEE Xplore and
AIP library packages.

Direct observation of exchange-driven spin interactions in one-dimensional system

Chengyu Yan,^{1,2,a)} Sanjeev Kumar,^{1,2,b)} Kalarikad Thomas,^{1,2,c)} Michael Pepper,^{1,2} Patrick See,³ Ian Farrer,^{4,d)} David Ritchie,⁴ J. P. Griffiths,⁴ and G. A. C. Jones⁴

¹London Centre for Nanotechnology, 17-19 Gordon Street, London WC1H 0AH, United Kingdom

²Department of Electronic and Electrical Engineering, University College London, Torrington Place, London WC1E 7JE, United Kingdom

³National Physical Laboratory, Hampton Road, Teddington, Middlesex TW11 0LW, United Kingdom

⁴Cavendish Laboratory, J.J. Thomson Avenue, Cambridge CB3 0HE, United Kingdom

(Received 8 June 2017; accepted 13 July 2017; published online 27 July 2017)

We present experimental results of transverse electron focusing measurements performed on an n-type GaAs based mesoscopic device consisting of one-dimensional (1D) quantum wires as injector and detector. We show that non-adiabatic injection of 1D electrons at a conductance of $\frac{e^2}{h}$ results in a single first focusing peak, which transforms into two asymmetric sub-peaks with a gradual increase in the injector conductance up to $\frac{2e^2}{h}$, each sub-peak representing the population of spin-state arising from the spatially separated spins in the injector. Further increasing the conductance flips the spin-states in the 1D channel, thus reversing the asymmetry in the sub-peaks. On applying a source-drain bias, the spin-gap, so obtained, can be resolved, thus providing evidence of exchange interaction induced spin polarization in the 1D systems. © 2017 Author(s). All article content, except where otherwise noted, is licensed under a Creative Commons Attribution (CC BY) license (<http://creativecommons.org/licenses/by/4.0/>). [<http://dx.doi.org/10.1063/1.4989374>]

Spintronics involves engineering the spin degrees of freedom to replace charges with spins to carry information precisely to meet the future technological challenges. This has led to a volume of theoretical¹ and experimental work on spin based systems, exploiting the spin-orbit interaction and the spin-Hall effect using low dimensional semiconductors and optical systems.²⁻⁷ Among various quantum systems, a simple yet powerful system is a one-dimensional (1D) quantum wire realised using a pair of split gates,⁸ resulting in the evolution of spin degenerate 1D subbands as the confinement potential is relaxed.⁹⁻¹¹ One of the merits of this system is that the spin degeneracy can be easily lifted on application of an in-plane magnetic field¹² such that spin-up and spin-down electrons could be energetically separated. However, it is also predicted that the exchange can induce partial spin polarization; in other words, it creates a spin-gap in the ground state of a longer 1D system.^{13,14} The origin of spin-gap in the 1D system has aroused a great interest to explain the “0.7 anomaly” in the framework of spin correlation between the 1D electrons.¹³⁻¹⁶

The spin polarization in a 1D quantum wire^{13,14} can be measured by means of transverse electron focusing (TEF),¹⁷⁻¹⁹ where the height of each focusing peak is proportional to the population of detected electrons. It has been confirmed experimentally in a GaAs hole gas^{20,21} and an InSb electron gas²² that the first focusing peak splits into two sub-peaks and each peak is associated with a spin of an electron. In this work, we provide direct evidence by means of focusing measurements

using electrons in the GaAs/AlGaAs heterostructure that the spin-gap can be detected precisely up to the first excited state in agreement with observations of the “0.7” and “1.7” structures.^{12,24} Furthermore, we show an effect in which spin repulsion due to the exchange interaction results in flip-flop of the spin-states. In addition, we have combined the source-drain bias spectroscopy with the focusing measurement and provide further evidence of the spin-gap in the 1D system.

The devices studied in the present work were fabricated from the high mobility two dimensional electron gas (2DEG) formed at the interface of the GaAs/Al_{0.33}Ga_{0.67}As heterostructure. At 1.5 K, the measured electron density (mobility) was $1.80 \times 10^{11} \text{ cm}^{-2}$ ($2.17 \times 10^6 \text{ cm}^2 \text{ V}^{-1} \text{ s}^{-1}$); therefore, the mean free path is over $10 \mu\text{m}$ which is much larger than the electron propagation length. The experiments were performed using a cryofree dilution refrigerator with a lattice temperature of 20 mK by the standard lockin technique.

The focusing device is specially designed so that the injector and the detector can be separately controlled to avoid a possible cross-talking between them using a 90° geometry.^{17,25} The linear focusing devices^{17,20-22,25} used in previous work share the center gate which may introduce a lateral electric field along the confinement direction. Figure 1 shows the experimental setup along with a typical focusing spectrum obtained using the device shown in the inset. The quantum wire used for the injector and detector has a width (confinement direction) of 500 nm and a length (current flow direction) of 800 nm. It may be noted that the quasi-1D quantum wire (in the regime defined between the injector and detector quantum wires, highlighted by the red arrow in Fig. 1) has a smaller lithographic size than the injector/detector quantum wires, and thus, within the studied injector/detector gate voltage, this quasi-1D quantum wire is in the pinch-off regime and so fully reflects the focused electrons.

^{a)}Electronic mail: uceeya3@ucl.ac.uk

^{b)}Electronic mail: sanjeev.kumar@ucl.ac.uk

^{c)}Currently at Department of Physics, Central University of Kerala, Riverside Transit Campus, Padannakkad, Kerala 671314, India.

^{d)}Currently at Department of Electronic and Electrical Engineering, University of Sheffield, Mappin Street, Sheffield S1 3JD, United Kingdom.

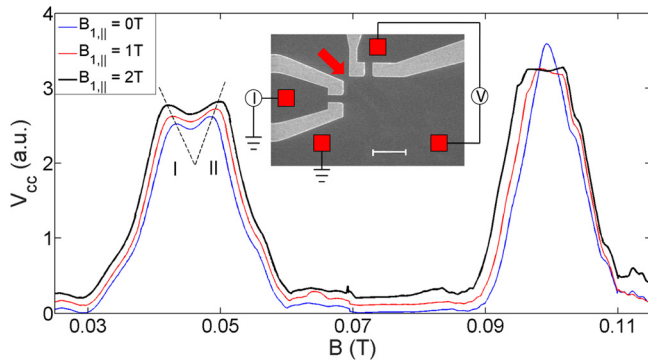


FIG. 1. The experiment setup and device characteristics. A representative plot of transverse electron focusing with both the injector and detector set to G_0 ($2e^2/h$). Periodic focusing peaks are well defined. The two sub-peaks have been highlighted as peak I and peak II in the paper. It is also shown that the splitting of focusing peaks is enhanced by in-plane magnetic field. The inset shows an SEM image of the device. The red squares are Ohmic contacts, whereas the left (top) pair of gray colored gates form the injector (detector) quantum wire. The lithographic defined width of the quantum wire is 500 nm and the length is 800 nm, and the separation between the injector and detector is 1.5 μm . The scale bar is 2 μm .

In the presence of a small positive transverse magnetic field B_\perp electrons are focused from the injector to detector, leading to focusing peaks periodic in B_\perp . The periodicity of 60 mT is calculated using the relationship¹⁷ $B_{focus} = \frac{\sqrt{2}\hbar k_F}{eL}$, where $\sqrt{2}$ accounts for the 90° geometry of the focusing device and is in good agreement with the experimental result. Here, e is the elementary charge, \hbar is the reduced Planck's constant, and L is the separation between the injector and detector.²⁶ Apart from the well resolved focusing peaks as shown in Fig. 1, it is interesting to note that the first focusing peak splits into two sub-peaks (denoted as peak I and peak II, respectively) while the second peak remains unsplit. The splitting of the first peak, not for the second peak, is predicted to be a sign of the spin-orbit interaction (SOI).^{18,19} It may be noted that the observed splitting of 5.5 mT (after scaling against L , it becomes 6.3 mT for 90° geometry) is much smaller than the 40 mT splitting in GaAs hole gas^{20,21} or 60 mT in InSb electron gas,²² which is expected for low SOI in n-GaAs. We made sure that the observed effect is not due to the disorder induced electron branching,²³ because the splitting of the first peak remained preserved when we swapped the role of the injector and the detector (see the discussion in the [supplementary material](#)). In addition, in the presence of in-plane magnetic field B_\parallel , the splitting of the first peak gets enhanced from 5.5 mT ($B_\parallel = 0$) to 8.3 mT ($B_\parallel = 2$ T), whereas the second peak started showing a tendency of splitting due to the Zeeman effect, thus confirming the effect to be spin related. Although the odd-peak splitting is a manifestation of SOI in 2DEG, the asymmetry of the two sub-peaks reflects the spin polarization of the injected 1D electrons.

A detailed study of focusing measurement as a function of injector conductance is shown in Fig. 2(a) where the detector is fixed in the middle of the first conductance plateau $G_0 = 2e^2/h$, and the injector conductance was varied from $0.4G_0$ (top trace) to $3.0G_0$ (bottom trace). In the lowest injector conductance regime ($0.4G_0 < G_i < 0.6G_0$), a single highly asymmetric peak occurs around 0.044 T; however, by

opening the injector further, a pronounced peak splitting is observed, resulting in sub-peaks I and II, which survive up to $2G_0$. It is important to note that the asymmetric single peak in the low injector conductance regime aligns with peak I rather than the central dip in the sub-peaks, suggesting that peak I represents a spin-state, and the absence of peak II emanates from the fact that the second spin state is not yet populated. In the large injector conductance regime (above $2G_0$), the two sub-peaks merge into a broad peak.

It is also worth mentioning that the intensity of two sub-peaks remains almost equal to each other when $G_i = G_0$, while an asymmetry in the sub-peak intensity was present elsewhere [Fig. 2(b)]. We argue that the sub-peaks of first focusing peak are associated with the two spin branches, as confirmed with the in-plane magnetic field result given in Fig. 1, while the asymmetry in the sub-peak intensity is a direct manifestation of spin polarization.^{18,19} The split in the focusing peak persists up to $2G_0$ which is consistent with the experimental observation of $1.7G_0$ in the conductance measurement which was attributed to spontaneous spin polarisation in the 1D system.^{12,24} The two spin states become degenerate at high injector conductance, resulting in a single broad peak for injector conductance $3G_0$. The peak height of sub-peaks I and II as a function of injector conductance is shown in Fig. 2(c). It may be noted that the intensity of peak I is higher than peak II for $G_i < G_0$; however, beyond G_0 , a swap in peak intensity is observed, i.e., at $1.2G_0$, the intensity of peak II is stronger than peak I, and at $2G_0$, both the peaks have almost similar magnitude. There is a tendency of a second intensity swap beyond $2G_0$.

A significant feature of the results is the alternation of the height of the spin-split peaks. We can account for this as the results here and elsewhere show that the 1D system has a tendency to spin alignment and a corresponding repulsion between spins. This introduces the spin-gap, and so, when the 1D channel widens, the second level ($2G_0$) starts to fill which then interacts with the polarised spins of the first level (G_0). As the minority spin band in the first level has a higher density of states (DOS) at the Fermi level than the majority spin band, the interaction tends to align the second level states with the minority spins of the first level. The net result is an alternation in the magnitude of the spin-split peaks as the channel is widened and the levels progressively become filled.

The observation of a single sub-peak I in low injector conductance regime ($G_i < 0.5G_0$) can be expressed in terms of DOS corresponding to a particular spin orientation, say spin-down [Fig. 2(d)]. As the injector conductance was gradually increased beyond $0.5G_0$ up to $0.9G_0$, the second spin state (subband) started getting populated, resulting in the observation of a major sub-peak I and a minor sub-peak II. The exchange interactions between the 1D electrons give rise to the repulsion between the two spin-states resulting in a spin-gap.¹³⁻¹⁵ The DOS for the spin-up state at $0.9G_0$, which has just emerged, will be less populated, so we see an asymmetry in the sub-peaks [Fig. 2(e)]. On further increasing the injector conductance to $1.2G_0$, the next DOS close to the Fermi level will have spin-up state as per the exchange theory (if not then the former and the latter ones will repel each other), and so, the population of spin-up state increases,

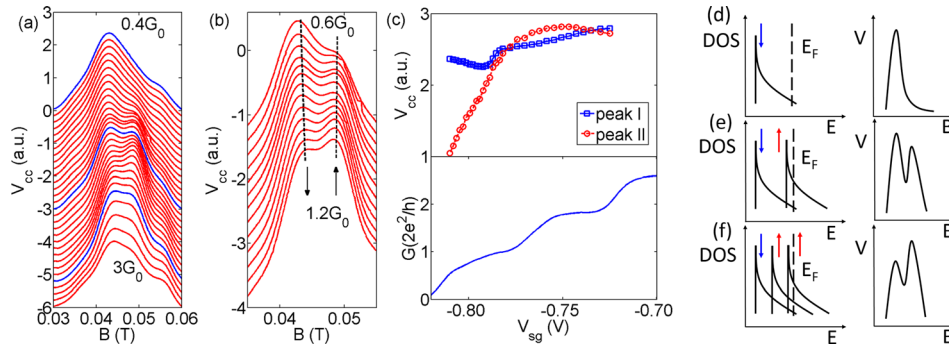


FIG. 2. TEF as a function of injector conductance. (a) Injector conductance was increased from $0.4G_0$ (top trace) to $3G_0$ (bottom trace). On opening the injector to $0.6G_0$, two sub-peaks started getting resolved, and merged to form a broad peak at $3G_0$. From top to bottom, the three highlighted blue traces were taken at $G_i = 0.4G_0$, G_0 , and $2G_0$, respectively. (b) Zoom-in of the data in (a) for $0.6G_0 < G_i < 1.2G_0$. The dotted lines are guide to the eye, reflecting the emergent alteration or flip-flop of the two spin states. Data in (a) and (b) have been offset vertically for clarity. (c) The intensity of peak I and peak II (top) against the injector conductance (bottom). (d)–(f) Schematic of the density of states (DOS, left) and the corresponding focusing peak (right) at $0.5G_0$, $0.9G_0$, and $1.2G_0$, respectively.

resulting a higher intensity of sub-peak II than sub-peak I. This situation is shown in Fig. 2(f) which is nothing but a flip of spin-states of Fig. 2(e).

We performed the focusing measurement by applying dc source-drain bias current in addition to an ac excitation current as shown in Fig. 3. The focusing result at different source-drain bias with the injector fixed at $0.5G_0$ is shown in Fig. 3(a). It was seen that with the positive bias current, a single focusing peak is observed, i.e., only sub-peak I appears. However, sub-peak I broadens along with the emergence of sub-peak II at the negative bias current. Figure 3(b) shows the focusing result at different bias currents with the injector fixed at G_0 . It was noticed that both the sub-peaks shift monotonically from the higher magnetic field end at -30 nA to the lower magnetic field side at 30 nA, which is consistent with the previous report²⁷ where such shift was attributed to the change in 2D Fermi wavevector k_F ; however, the absolute value of splitting remains almost the same, regardless of the bias current. It is interesting to note that the focusing spectrum eventually evolves into a single asymmetric sub-peak I with a bias current of 30 nA. The observation of spin-gap requires a small current bias; otherwise, electron heating at larger bias will result in broadening of the focusing peaks.²⁷

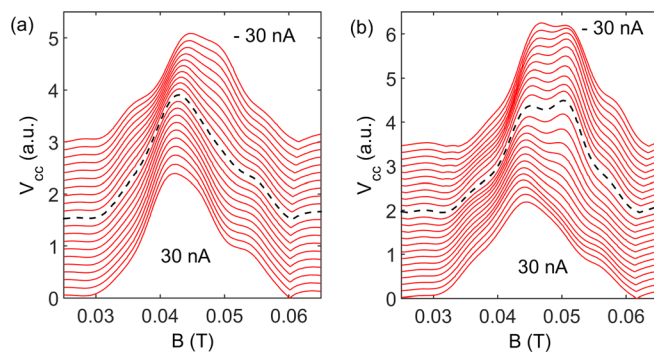


FIG. 3. TEF with source-drain bias current. (a) Result for the injector fixed at $G_i = 0.5G_0$, a broad asymmetric peak I along with the emergence of peak II is observed with negative bias current (from the dashed trace to top trace) while a sharp peak I is present with positive bias current (from the dashed black trace to bottom trace). (b) Result for injector fixed at $G_i = G_0$, the peak splitting is unaffected with negative bias current while a single asymmetric peak is observed with large positive bias current.

The source-drain dependence data can be understood using the spin-gap model as shown in Fig. 4. In the transverse electron focusing configuration, the drain reservoir is always grounded, and thus, we assume that the drain chemical potential μ_d remains the same, regardless of the bias current; on the contrary, the source chemical potential μ_s changes monotonically in the presence of the bias current. The negative bias current pushes μ_s upwards (energy increases) while positive bias current pushes it downwards (energy reduces). For $G_i = 0.5G_0$, μ_s sits in the spin-gap [position I in Fig. 4(a)], and thus, only the lower spin-subband is populated because the intensity of the focusing peak is directly proportional to the population of injected electrons;¹⁷ therefore, only peak I is observed. The positive bias current pushes μ_s downwards even further (position II) so that higher spin-subband gets even less chance to be populated, and the single focusing peak persists. On the other hand, the negative bias current pushes μ_s upwards (position III), and hence, the higher spin-subband starts getting activated, and peak II gradually appears; however, the intensity of peak II is smaller than that of peak I because the higher spin subbands is partially populated while the lower spin subband is fully occupied unless μ_s is pushed above the higher subband. For $G_i = G_0$, μ_s is above both the spin-subbands at zero source-drain bias [position IV in Fig. 4(b)], so both the spin-subbands are populated, resulting in two sub-peaks. Both the subbands will be populated when μ_s is pushed upwards (negative bias, position VI); however, the situation will be different when μ_s is

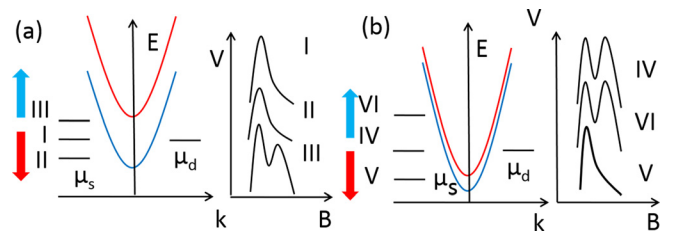


FIG. 4. Spin-gap model for TEF. (a) The injector is set to $0.5G_0$; at zero bias current μ_s is at position I and only peak I is present. Positive bias current (bold red arrow) pushes μ_s downward to position II, still only peak I appears; negative bias current (bold blue arrow) pushed μ_s upward to position III so that peak II starts getting resolved while peak I is pronounced. (b) The injector is set to G_0 ; both peaks I and II are observable at position IV and VI, while only peak I is present at position V.

pushed into the spin-gap with a relatively large positive bias current (i.e., position V), where only one spin subband can be populated which in turn results in a single peak.

From the model, it is found that peaks I and II correspond to lower and higher spin subbands, which is also revealed in Fig. 2 as peak II slowly builds up when the injector conductance was increased to $2G_0$. Increasing conductance by making the gate voltage less negative pushes both higher and lower spin subbands downward with respect to μ_s ; thus, lower spin subband is populated first, and then, the higher spin subband is populated in the large conductance regime.

In conclusion, we show that non-adiabatic injection of 1D electrons whose spins have been spatially separated on the 2D regime can be detected in the form of a split in the first focusing peak, where sub-peak I (II) represents the lower (upper) spin state. Combining transverse electron focusing with source-drain bias spectroscopy clearly shows that a spin-gap is inherently present in n-GaAs which is driven by the exchange and correlation between the 1D electrons. The spin-gap persists up to the first excited state in agreement with the previous conductance measurement. Our results show that such spin properties of 1D electrons may have potential usages in future spintronics devices.

See [supplementary material](#) for additional experimental data in different focusing configurations.

We thank Professor K. Berggren for many fruitful discussions. The work was funded by the Engineering and Physical Sciences Research Council (EPSRC), UK.

¹H. Dery and L. J. Sham, *Phys. Rev. Lett.* **98**, 046602 (2007).

²S. Datta and B. Das, *Appl. Phys. Lett.* **56**, 665 (1990).

³S. D. Sarma, J. Fabian, X. Hu, and I. Žutić, *Solid State Commun.* **119**, 207–215 (2001).

⁴I. Žutić, J. Fabian, and S. D. Sarma, *Rev. Mod. Phys.* **76**, 323–410 (2004).

⁵B. Behin-Aein, D. Datta, S. Salahuddin, and S. Datta, *Nat. Nanotechnol.* **5**, 266–270 (2010).

⁶J.-F. Liu, K. S. Chan, and J. Wang, *Appl. Phys. Lett.* **101**, 082407 (2012).

⁷J. Wunderlich, B.-G. Park, A. C. Irvine, L. P. Zârbo, E. Rozkotová, P. Nemeč, V. Novák, J. Sinova, and T. Jungwirth, *Science* **330**, 1801–1804 (2010).

⁸T. J. Thornton, M. Pepper, H. Ahmed, D. Andrews, and G. J. Davies, *Phys. Rev. Lett.* **56**, 1198–1201 (1986).

⁹D. Wharam, T. J. Thornton, R. Newbury, M. Pepper, H. Ahmed, J. E. F. Frost, D. G. Hasko, D. C. Peacock, D. A. Ritchie, and G. A. C. Jones, *J. Phys. C: Solid State Phys.* **21**, L209 (1988).

¹⁰B. J. van Wees, H. van Houten, C. W. J. Beenakker, C. W. J. Beenakker, J. G. Williamson, L. P. Kouwenhoven, D. van der Marel, and C. T. Foxon, *Phys. Rev. Lett.* **60**, 848–850 (1988).

¹¹C. Yan, S. Kumar, M. Pepper, P. See, I. Farrer, D. Ritchie, J. Griffiths, and G. Jones, *Phys. Rev. B* **95**, 041407 (2017).

¹²K. J. Thomas, J. T. Nicholls, M. Y. Simmons, M. Pepper, D. R. Mace, and D. A. Ritchie, *Phys. Rev. Lett.* **77**, 135–138 (1996).

¹³C.-K. Wang and K.-F. Berggren, *Phys. Rev. B* **54**, R14257–R14260 (1996).

¹⁴C.-K. Wang and K.-F. Berggren, *Phys. Rev. B* **57**, 4552–4556 (1998).

¹⁵D. J. Reilly, T. M. Buehler, J. L. O'Brien, A. R. Hamilton, A. S. Dzurak, R. G. Clark, B. E. Kane, L. N. Pfeiffer, and K. W. West, *Phys. Rev. Lett.* **89**, 246801 (2002).

¹⁶H. Bruus, V. V. Cheianov, and K. Flensberg, *Physica E* **10**, 97–102 (2001).

¹⁷H. van Houten, C. W. J. Beenakker, J. G. Williamson, M. E. I. Broekaart, P. H. M. van Loosdrecht, B. J. van Wees, J. E. Mooij, C. T. Foxon, and J. J. Harris, *Phys. Rev. B* **39**, 8556–8575 (1989).

¹⁸G. Usaj and C. A. Balseiro, *Phys. Rev. B* **70**, 041301 (2004).

¹⁹A. Reynoso, G. Usaj, and C. A. Balseiro, *Phys. Rev. B* **75**, 085321 (2007).

²⁰L. P. Rokhinson, L. N. Pfeiffer, and K. W. West, *Phys. Rev. Lett.* **96**, 156602 (2006).

²¹S. Chesi, G. F. Giuliani, L. P. Rokhinson, L. N. Pfeiffer, and K. W. West, *Phys. Rev. Lett.* **106**, 236601 (2011).

²²A. R. Dedigama, D. Deen, S. Q. Murphy, N. Goel, J. C. Keay, M. B. Santos, K. Suzuki, S. Miyashita, and Y. Hirayama, *Physica E* **34**, 647–650 (2006).

²³D. Maryenko, F. Ospald, K. v. Klitzing, J. H. Smet, J. J. Metzger, R. Fleischmann, T. Geisel, and V. Umansky, *Phys. Rev. B* **85**, 195329 (2012).

²⁴F. Stigakis, C. J. B. Ford, M. Pepper, M. Kataoka, D. A. Ritchie, and M. Y. Simmons, *Phys. Rev. Lett.* **100**, 026807 (2008).

²⁵R. M. Potok, J. A. Folk, C. M. Marcus, and V. Umansky, *Phys. Rev. Lett.* **89**, 266602 (2002).

²⁶C. Yan, S. Kumar, K. J. Thomas, M. Pepper, P. See, I. Farrer, D. Ritchie, J. Griffiths, and G. Jones, “Gate tunable injection and detection of spin states in one-dimension” (unpublished).

²⁷R. I. Hornsey, J. R. A. Cleaver, and H. Ahmed, *Phys. Rev. B* **48**, 14679–14682 (1993).